Progress In Electromagnetics Research M, Vol. 39, 11–18, 2014

Multimode Analysis and PIC Simulation of a Metal PBG Cavity Gyrotron Oscillator

Ashutosh Singh[1, 2, *] and Pradip K. Jain[2]

Abstract—This paper is devoted to the study of beam-wave interaction behavior of a 35 GHz photonic band gap (PBG) cavity gyrotron operating in a higher order $TE_{3,4,1}$ mode. For the present gyrotron, PBG cavity is used instead of conventional tapered cylindrical cavity due to its promising feature of the mode selectivity. In order to observe beam-wave interaction behavior, multimode theory has been used for the PBG cavity operating at the fundamental harmonic mode. Results obtained from the analysis have been validated using a commercially available 3D PIC code. The energy and phase variations of electrons demonstrate the bunching mechanism as well as energy transfer phenomena. RF power output obtained from the analysis as well as PIC simulation is compared and is found in close agreement within 12%. More than 45 kW of stable RF power output is achieved in $TE_{3,4,1}$ mode with $\sim 17\%$ efficiency. The existence of competing modes has been considerably reduced, and the single mode operation of PBG cavity gyrotron has been achieved.

1. INTRODUCTION

Gyrotrons are capable of generating high power coherent electromagnetic radiation in millimeter, submillimeter and terahertz wave regime, both in the pulse as well as CW operations [1–3]. Gyrotrons have various technological and scientific applications, such as electron cyclotron resonance plasma heating (ECRH), materials processing, radar systems, dynamic nuclear polarization enhanced nuclear magnetic resonance and electron spin resonance spectroscopy, medical imaging and particle accelerations [3, 4].

High frequency gyrotrons are also attractive for variety of new applications. Approaching towards higher frequency of gyrotron operation leads to the shrinkage of cavity structure dimension. Consequently, various problems arise due to the increase in heat load on the cavity walls, beam interception and fabrication difficulties; hence overmoded cavities are used to surmount these problems. Additionally, for such higher frequency, larger magnetic field is required for the fundamental mode of operation [5–7]. These constraints limit the design of conventional cylindrical cavities at these frequencies. In such case, the photonic band gap (PBG) cavity is useful in comparison to the conventional cylindrical cavity. The overmoded cylindrical cavity can switch into parasitic mode of oscillations leading to performance degradation [7]. By using mode selectivity and choosing the appropriate operating parameters, mode competition can be successfully eliminated.

PBG structures have shown promising performances as having the ability of controlling the electromagnetic wave propagation. Several gyro-devices have been reported in the past utilizing the attributes of PBG structures, such as, gyrotron, high gradient accelerator, backward wave oscillator and traveling wave tube (TWT) and Gyro-TWT amplifier [7–12]. Sirigiri et al. has designed a 140 GHz gyrotron using PBG cavity and experimentally demonstrated its performance [7]. A second cyclotron

Received 21 August 2014, Accepted 15 September 2014, Scheduled 25 September 2014

* Corresponding author: Ashutosh Singh (asingh.rs.ece@iitbhu.ac.in).

[1] Faculty of Physical Sciences, Institute of Natural Sciences and Humanities, Shri Ramswaroop Memorial University, Lucknow-Deva Road, U. P. 225003, India. [2] Center of Research in Microwave Tubes, Department of Electronics Engineering, Indian Institute of Technology (Banaras Hindu University), Varanasi 221005, India.

harmonic PBG cavity gyrotron operating in the $TE_{3,4,1}$ mode has been analyzed by Li et al. using nonlinear analysis [9]. They successfully demonstrated the complete elimination of mode competition in the PBG cavity. Nanni et al. has implemented the PBG waveguide as an interaction structure in a 250 GHz gyro-TWT in order to utilize the merit of mode selectivity [12].

The RF behavior of a 35 GHz PBG cavity gyrotron operating in $TE_{3,4,1}$ mode is studied using the multimode analysis and the PIC simulation code. The design procedure and beam absent behaviour of the PBG cavity has already been reported [13]. Here, the beam present behaviour of the PBG cavity is studied. The time dependent nonlinear multimode theory has been used to observe the RF behavior in the presence of all competing modes. The beam-wave interaction behaviour is also observed using commercially available PIC simulation code 'CST Particle Studio'. The cavity operation is monitored to predict the desired frequency and mode of operation. Velocity spread is taken zero in the theory as well as simulation. Temporal signal growth and output power of designed mode as well as the possible competing modes is observed and the comparison of their amplitudes is discussed. Results obtained from the multimode analysis have been validated with those obtained through the PIC simulation.

2. TIME DEPENDENT MULTIMODE THEORY

In order to study the RF performance of an overmoded cavity, multimode theory is used here based on Fliflet et al.'s formulation [14]. The coupled equations of electron momentum and phase are solved using the Runge-Kutta method and these values are further used in solving the coupled equations of RF amplitude and phase. Small initial amplitude is assigned for each mode with arbitrary phase to initiate the numerical integration. The coupled equations of RF amplitude and phase are integrated for all modes iteratively at each time step. Finally, the information of temporal amplitude and phase leads to the evaluation of the RF power growth. A Matlab code has been developed for the evaluation of temporal power growth. The PBG cavity for the confined mode is treated as similar to the conventional tapered cylindrical cavity and defect radius has been considered analogous to radius of the cylindrical cavity. This approximation is valid only for the confined modes. One of the major differences is the diffractive quality factor (Q_D). There is a finite iris between the PBG cavity and output taper that leads to higher Q_D. This Q_D value has been measured using "CST microwave studio" code and has been used in Fliflet's theory for calculating RF power output. The Gaussian shaped axial field profile is considered along the PBG cavity. The electron beam parameters are calculated using nonlinear analysis as listed in Table 2 [15].

3. RESULTS AND DISCUSSION

In the eigenmode analysis, two modes $TE_{3,4}$ and $TE_{1,5}$ were observed in the forbidden band of PBG structure and hence, $TE_{1,5}$ is taken as a strong mode competitor [13]. To obtain the electron beam parameters, coupling coefficient and start oscillation current diagram are estimated using linearized single-mode theory for the fundamental harmonic (Figure 1) [1]. Plus (+) and minus (−) sign denote the counter and co-rotating modes, respectively. Coupling coefficient gives the information regarding selection of beam radius for the maximum coupling in the designed mode and also to avoid the mode competition. Here, maximum coupling took place at normalized 0.364 therefore the electron beam is kept at this beam radius (Figure 1(a)). From Figure 1(b), 4 A beam current is chosen so that only desired co-rotating $TE_{3,4}$ mode would oscillate in the cavity.

3.1. Multimode Theory

The output power for $TE_{3,4}$ and $TE_{1,5}$ modes are shown in Figure 2 for 1.37 T magnetic field of and 4 A beam current. A stabilized 45 kW of output power is obtained in the design mode after 90 ns while other modes have few milliwatts only. Hence, only single $TE_{3,4}$ mode excitation takes place in the PBG cavity. In the cylindrical cavity, presence of competing modes are inevitable and due to slight change in electron beam parameters, the cavity may switch to oscillate into any other nearby parasitic mode that leads to the device instability and poor efficiency. There are several reasons to alter the electron beam parameters such as, beam loading, beam velocity spread, etc.. On the other hand, for PBG cavity case,

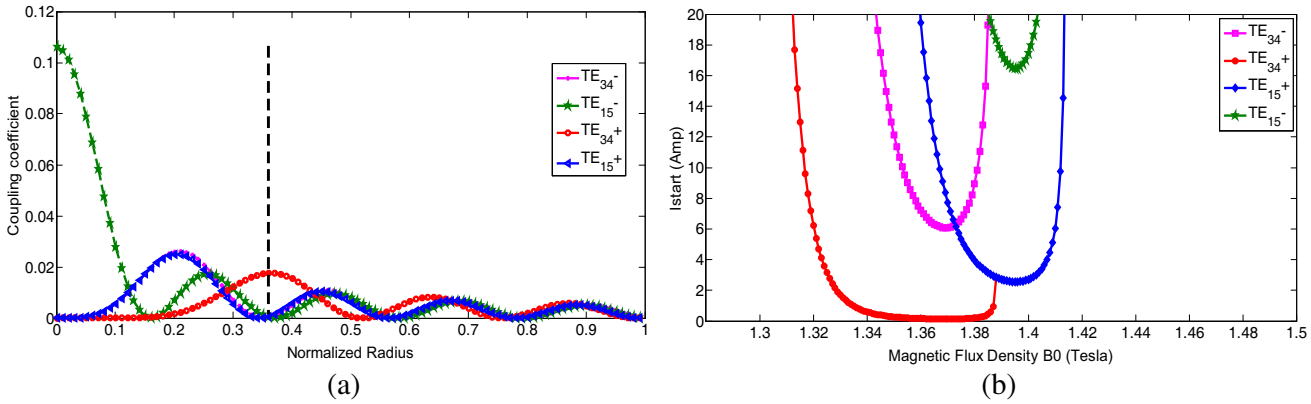

Figure 1. (a) Coupling coefficient with normalized radius of electron beam, and (b) start oscillation current with magnetic flux density (B_0).

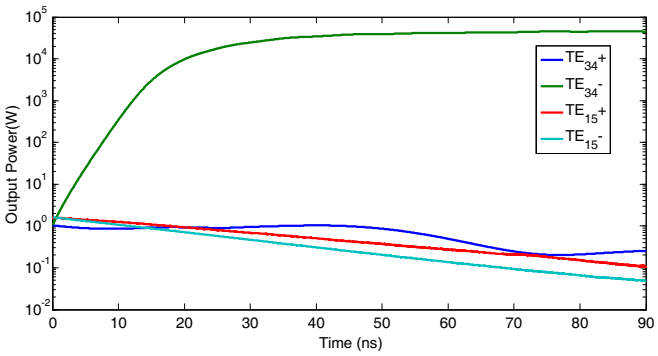

Figure 2. Temporal growth of output power for $TE_{3,4,1}$ mode with all competing modes in the PBG cavity at magnetic field $(B_0) = 1.37\,\mathrm{T}$.

the competing modes do not exist in the cavity and hence even by altering the beam parameters, mode switching does not occur.

The momentum and phase of all the particles with respect to the axial distance are shown in Figure 3. At the entrance of the RF cavity, particles of each beamlet have zero electron momentum and its phase is equally distributed between 0 and 2π. As the particles move along the axial direction, normalized momentum and phase of all the particles get perturbed due to the electrons interaction with RF. At the output end of the cavity, net momentum of all the electrons is decreased and hence energy transfer to the RF takes place.

3.2. PIC Simulation

A 3D model of interaction structure is used in the PIC simulation, as shown in Figure 4(a). The PBG cavity dimension is given in Table 1. Input and output taper is provided to maintain standing wave pattern in the cavity. Boundary conditions are made electric ($E_t = 0$) along all six faces of the PBG cavity. Hexahedral meshing is used in the simulation. Proper meshing of structure is desirous to obtain the converging results with sufficient accuracy. Gyrating electron beam is produced by special arrangement and is injected from the input taper end into the interaction structure. 12 numbers of beamlets are typically considered that provides sufficient accurate results. A uniform DC magnetic field of 1.36 T is applied along the interaction structure (Figure 4(b)). The designed PBG cavity is simulated in the beam absent and the beam present cases. Beam absent simulation has been performed to observe the existence of possible modes and has been reported earlier [13]. A well confined $TE_{3,4}$ mode along with a $TE_{1,5}$ competing mode was observed. Here, the beam present case is explored to observe the beam-wave interaction behavior.

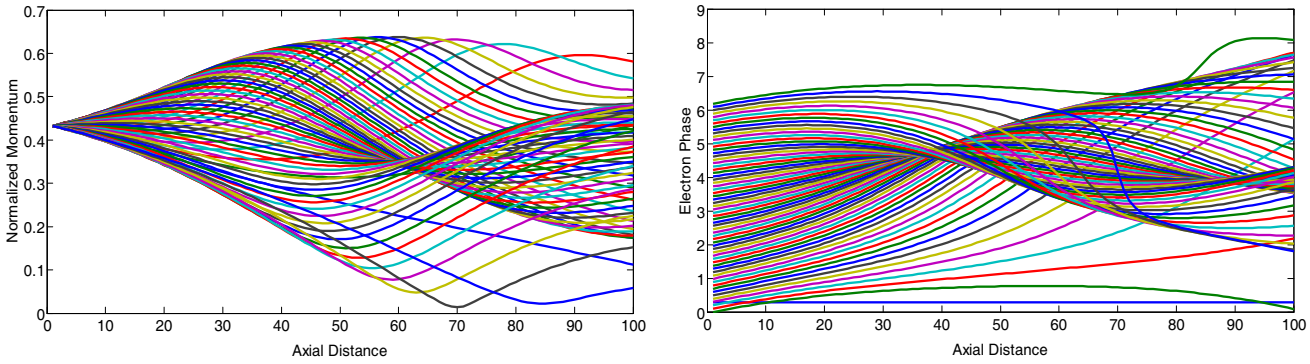

(a) (b)

Figure 3. Variation of normalized momentum and phase along axial distance of the PBG cavity.

Table 1. Geometry parameters of the PBG cavity.

Particulars	**Specifications**
Downtaper length (L_{down})	30 mm
Cavity length (L_{cavity})	44 mm
Uptaper length (L_{up})	46 mm
Downtaper angle	3.5°
Uptaper angle	4.5°
Rod radius (r)	4.93 mm
Lattice constant (a)	14.33 mm
r/a ratio	0.344
Normalised frequency (fa/c)	1.672

Table 2. Electron beam parameters of the PBG cavity gyrotron.

Particulars	**Specifications**
Mode	$TE_{3,4,1}$
Frequency f	35 GHz
Harmonic number n	1
Accelerating voltage V_0	65 kV
Beam current I_0	4 A
Velocity ratio α	1.5
Magnetic field B_0	1.36 T
Wall radius r_w	19.9 mm
Beam radius r_b	7.25 mm
Diffractive Q_D	6200

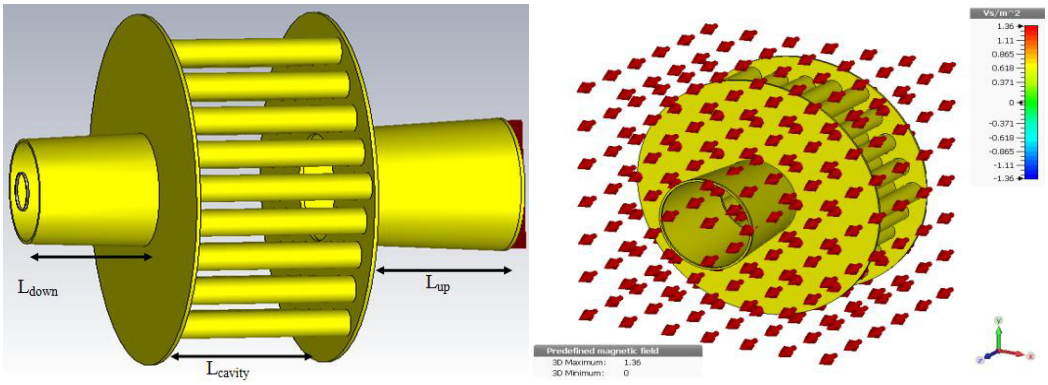

(a) (b)

Figure 4. (a) 3D Model of PBG cavity used in the PIC simulation and (b) homogeneous DC magnetic field distribution along the PBG cavity.

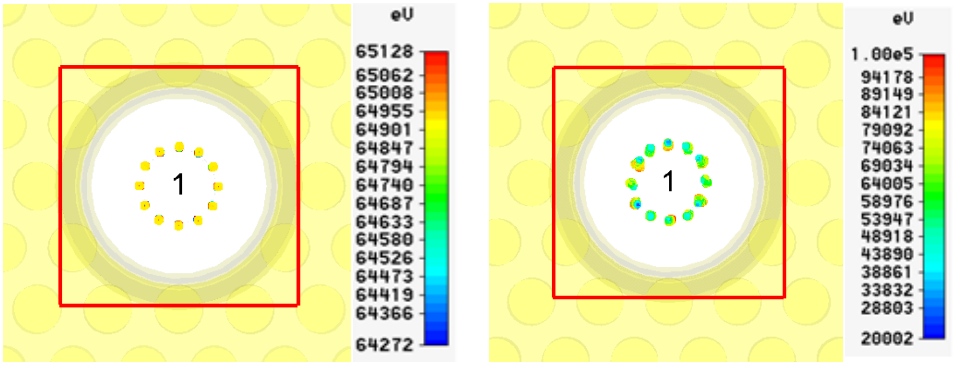

(a) (b)

Figure 5. Profile of beamlets (a) before and (b) after the beam-wave interaction.

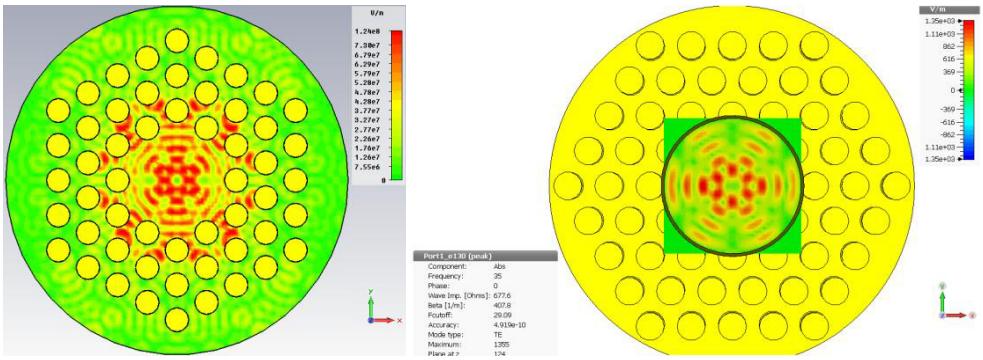

(a) (b)

Figure 6. (a) Electric field distribution at the mid plane of the PBG cavity and (b) $TE_{3,4}$ mode at waveguide port at uptaper end.

In the beam present case, a gyro-magnetic electron beam of 65 keV is introduced at the left end of the confining interaction structure to introduce the oscillations inside the PBG cavity. In Figure 5, the front view of beamlets (from the uptaper end of the interaction structure) is shown before and after the beam-wave interaction. Obviously, the energy of all the particles is same before interaction and the particles lie in the equal radii of Larmor orbit. After the interaction, bunching of electrons takes place and this electron bunch transfer its energy to the RF field in a decelerating phase. The electric field at the mid plane of the PBG cavity is monitored as shown in Figure 6(a). Obviously, the cavity operates in $TE_{3,4,1}$ mode at 34.5 GHz. For the confined mode in the PBG cavity, it can be seen that the field slightly penetrates into the rod region and radius considered analytically is smaller than actual one. This difference can be of the order of lattice constant. The $TE_{3,4,1}$ mode at the output taper waveguide port is shown in Figure 6(b). The energy of all particles along the axis of PBG cavity is shown in Figure 7(a). At the input down taper side, all the particles have same 65 keV of energy. As the electrons traverse into the interaction structure, beam-wave interaction phenomena takes place and the energy of all the particles get perturbed. At the output end of PBG cavity, majority of electrons come down to 65 keV energy level that represents a net energy transfer from electron beam to RF.

A probe is placed inside the cavity to record the temporal response of electric field. The Fourier transform of this time signal provides frequency characteristics of the cavity operation as shown in Figure 7(b). Obviously, cavity operates nearly at 34.5 GHz resonant frequency. Temporal signal amplitudes are observed related to the $TE_{3,4}$ and $TE_{1,5}$ modes at the waveguide port of uptaper end (Figure 8(a)). Obviously, signal growth in $TE_{3,4}$ mode is higher than that of $TE_{1,5}$ mode. Hence, $TE_{1,5}$ mode, which has almost negligible value of amplitude, is not able to grow in the PBG cavity.

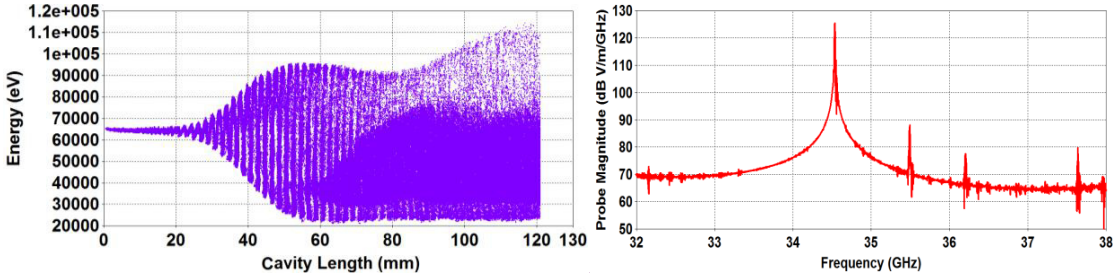

Figure 7. (a) Energy distribution of all the particles along the cavity length and (b) frequency spectrum of probe signal placed inside the cavity.

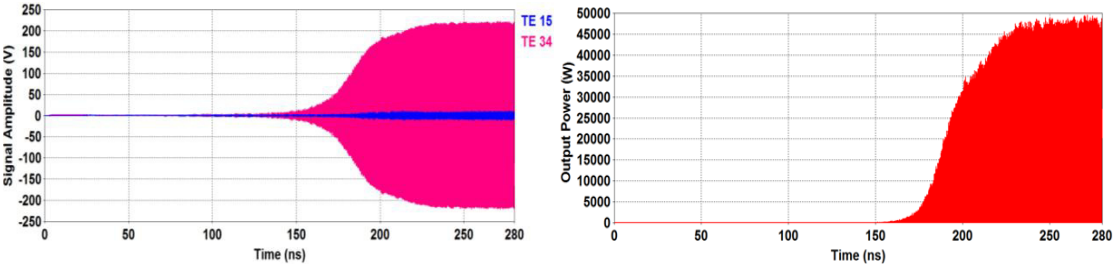

Figure 8. (a) Temporal signal amplitudes of $TE_{3,4}$ and $TE_{1,5}$ modes and (b) temporal output power growth in $TE_{3,4}$ mode at uptaper end of the PBG cavity.

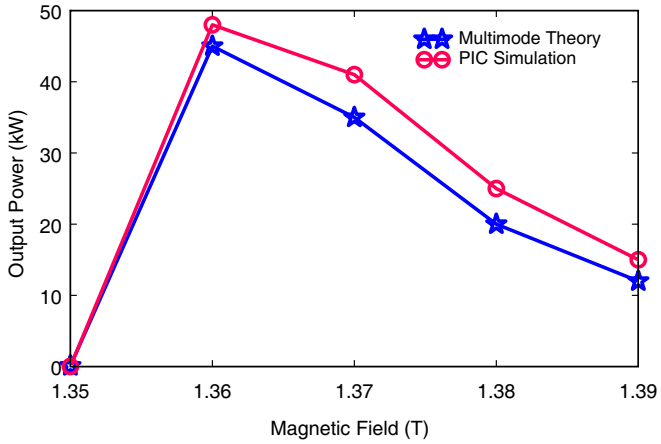

Figure 9. Comparison of output powers obtained from multimode theory and PIC simulation.

The cavity takes around 230 ns in establishing the $TE_{3,4}$ mode and after this, signal amplitude becomes stable. This consistent power level supports a stable performance of the gyrotron. The saturation time is different in both theory as well as simulation. The possible reason behind this may be that the time scale of change in amplitude and phase of a mode in the cavity is larger than time scale in which particle's orbits change. In the multimode analysis, this fact has been exploited which control the computation time significantly. On the other hand, in PIC code, no such provision is known to exploit the order of time scales and the interaction process evolves accurately and self-consistently. The temporal RF power output is also estimated related to the $TE_{3,4}$ mode (Figure 8(b)). The output power saturates after 230 ns and reaches to a peak value of around 48 kW with 18.5% efficiency. This output power and efficiency in PBG cavity case is smaller compared to cylindrical cavity because Q_D is

higher for PBG cavity. Hence, more power is absorbed in the PBG cavity on the contrary to cylindrical cavity.

The RF power output computed using multimode analysis is compared with the simulated values (Figure 9). It can be seen that the results obtained from the multimode analysis and PIC simulation are in close agreement within $\sim 12\%$. This difference is probably due to the variation in radius of the PBG cavity considered in both theory as well as simulation. From the beam absent and beam present approaches, it is established that the designed PBG cavity is operating in a single mode without any significant mode competition.

4. CONCLUSION

In the present paper, RF behavior of a 35 GHz photonic band gap (PBG) cavity made of triangular lattice of metallic rods has been analyzed using the time dependent multimode analysis as well as the PIC simulation. The designed PBG cavity is able to operate into a single mode and the mode competition is eliminated. Using the multimode analysis, around 45 kW RF power output has been obtained in the $TE_{3,4,1}$ mode with $\sim 17\%$ efficiency. In the PIC simulation, a well confined $TE_{3,4,1}$ mode has been observed in the PBG cavity at 34.54 GHz with no mode competition. The energy distribution of all the particles along the interaction length represents a net energy transfer from the electron beam to the RF field. The cavity takes some time to settle in $TE_{3,4}$ mode from the background noise and finally after 230 ns, a stable 48 kW output power has been obtained. The frequency spectrum of the recorded field has a single peak at 34.5 GHz that confirms the device is intended to operate at 34.5 GHz resonant frequency. The output power obtained from multimode analysis and PIC simulation is in close agreement within $\sim 12\%$. The PIC simulation presented here shows an extensive demonstration of beam-wave interaction mechanism in PBG cavity gyrotron. This present work would be helpful in the designing PBG cavity gyrotron operating in the higher order mode and higher frequency.

REFERENCES

1. Kartikeyan, M. V., E. Borie, and M. K. Thumm, *Gyrotrons: High Power Microwave and Millimeter Wave Technology*, Springer, Germany, 2004.
2. Rzesnicki, T., B. Piosczyk, S. Kern, S. Illy, J. Jianbo, A. Samartsev, A. Schlaich, and M. Thumm, "2.2-MW record power of the 170-GHz European preprototype coaxial-cavity Gyrotron for ITER," *IEEE Transactions on Plasma Science*, Vol. 38, No. 6, 1141–1149, 2010.
3. Thumm, M., "State-of-the-art of high power gyro-devices and free electron masers, update 2011," Forschungszentrum Karlsruhe, Germany, Scientific Reports FZKA 7467, 2012.
4. Hornstein, M. K., V. S. Bajaj, R. G. Griffin, and R. J. Temkin, "Continuous wave operation of a 460-GHz second harmonic gyrotron oscillator," *IEEE Trans. Plasma Science*, Vol. 34, 524–533, 2006.
5. Kreischer, K. E., R. J. Temkin, H. R. Fetterman, and W. J. Mulligan, "Multimode oscillation and mode competition in high-frequency gyrotrons," *IEEE Trans. Microwave Theory Tech.*, Vol. 32, 481–490, 1984.
6. Liu, P. K. and E. Borie, "Mode competition and self-consistent simulation of a second harmonic gyrotron oscillator," *Int. J. Infrared Millimeter Waves*, Vol. 21, No. 6, 855882, 2000.
7. Sirigiri, J. R., K. E. Kreischer, J. Macuhzak, I. Mastovsky, M. A. Shapiro, and R. J. Temkin, "Photonic band gap resonator Gyrotron," *Phys. Rev. Lett.,* Vol. 86, 5628–5631, 2001.
8. Jang, K.-H., S.-G. Jeon, J.-I. Kim, J.-H. Won, J.-K. So, S.-H. Bak, A. Srivastava, S.-S. Jung, and G.-S. Park, "High order mode oscillation in a terahertz photonic-band-gap multibeam reflex klystron," *Appl. Phys. Lett.*, Vol. 93, 211104, 2008.
9. Liu, G., X. Chen, and C. Tang, "Design of a second cyclotron harmonic gyrotron oscillator with photonic band-gap cavity," *J. Phys. D: Appl. Phys.*, Vol. 44, 295102 (7pp), 2011.
10. Smirnova, E. I., A. S. Kesar, I. Mastovsky, M. A. Shapiro, and R. J. Temkin, "Demonstration of a 17-GHz, high-gradient accelerator with a photonic-band-gap structure," *Phys. Review Lett.*, Vol. 95, 074801, 2005.

11. Gao, X., Z. Yang, Y. Xu, L. Qi, D. Li, Z. Shi, F. Lan, and Z. Liang, "Dispersion characteristic of a slow wave structure with metal photonic band gap cells," *Nuclear Instruments and Methods in Physics Research A*, Vol. 592, 292–296, 2008.
12. Nanni, E. A., M. A. Shapiro, and R. J. Temkin, "A 250 GHz photonic band gap gyrotron traveling wave amplifier," *IEEE Thirteenth International Vacuum Electronics Conference* (*IVEC*), 413–414, Monterey, CA, 2012.
13. Singh, A. and P. K. Jain, "Eigenmode analysis of metal photonic band gap cavity for Gyrotron operating in higher order mode," *PIERS Proceedings*, 1734–1738, Kuala Lumpur, Malaysia, Mar. 27–30, 2012.
14. Fliflet, A. W., R. C. Lee, S. H. Gold, W. M. Manheimer, and E. Ott, "Time-dependent multimode simulation of gyrotron oscillators," *Phys. Rev. A*, Vol. 43, No. 11, 6166–6176, Jun. 1991.
15. Danly, B. G. and R. J. Temkin, "Generalized nonlinear harmonic gyrotron theory," *Physics of Fluids,* Vol. 29, 561–567, 1986.